Third order aberration spots of holographic lenses

J. Masajada, J. Nowak

Institute of Physics, Technical University of Wrocław, Wybrzeże Wyspiańskiego 27, 50-370 Wrocław, Poland.

The third order aberration spots for spherical aberration and coma in the case of holographic lenses recorded on quadrics of revolution were investigated. The investigations were made numerically and, if possible, analytically. The formulas for the third order aberrations in the case of holograms recorded on a plane substrate and readout on the cylindrical substrate were derived. The aberration spots of holographic lenses in this case were also investigated.

1. Introduction

The holographic optical elements (HOE) are more and more important in modern optics. The holographic lenses (holo-lenses) are the HOEs most frequently used in practice. Holograms (holo-lenses are special kind of hologram) recorded on the plane and spherical substrate are well described [1]–[5]. Recording holo-lenses on spherical substrate we can improve image quality. The proper radius of spherical substrate allows us to compensate coma without any influence on correction of spherical aberration. Astigmatism, field curvature and distortion do not depend on substrate geometry. Coma correction causes the aberration spot to be symmetrical. Image quality improvement, however, is still not satisfied. For this reason, we tried to get better improvement by using other quadrics of revolution as holo-lens substrate. The aberrations of hologram recorded on quadrics of revolution (quadrics) are described in papers [6]–[9].

In this paper we want to analyse the influence of quadrics substrate on the aberration spot shape. The holo-lens aberrations are usually described in the expansion given by MEIER [3] which is analogous to that used in classical optics. In the case of holo-lens such an approximation is precise enough, and more useful than one given by CHAMPAGNE [2] for the general case of hologram.

2. Analytical formulas

The eikonal for the third order aberrations recorded on quadrics in the Meier's expansion is given by equation [9]

$$W = -\frac{1}{8}\alpha^2 S - \frac{1}{4}\alpha\beta G - \frac{1}{8}\beta^2 S_p - \frac{1}{2}A_x - \frac{1}{2}A_y - \frac{1}{2}A_{xy} + \frac{1}{2}\alpha x C_x$$

$$+ \frac{1}{2}\alpha y C_y + \frac{1}{2}\beta x C_{px} + \frac{1}{2}\beta y C_{py} - \frac{1}{4}\alpha F - \frac{1}{4}\alpha\beta F_p + \frac{1}{2}x D_x + \frac{1}{2}y D_y \qquad (1)$$

where: S, S_p, G, A_x, A_{xy}, C_x, C_y, C_{px}, C_{py}, F, F_p, D_x, D_y are the aberrations coefficients; α, β are the parameters describing the substrate geometry. We want to deal with holo-lens recorded on the sphere, ellipsoid, paraboloid, hyperboloid and cylinder in comparison with the holo-lens recorded on a plane substrate.

The quadrics are given by equation

$$z = 1/2 C(x^2 + \sigma y^2 + \varepsilon z^2) \tag{2}$$

where: C, ε, σ are parameters of the surface.

i) Sphere, ellipsoid, hyperboloid of one sheet
   The coefficients α, β are of the form:

$$\alpha = 2(C\varepsilon)^{-2}[1 - (1 - C^2 r^2 \varepsilon)^{-1/2}], \tag{3}$$

$$\beta = r^2(1 - 1/\varepsilon) \tag{4}$$

where $r^2 = x^2 + y^2$.

Since we consider the third order approximation, we can apply it to the square root in Eq. (3). We get

$$\alpha_a = r^2 \varepsilon^{-1}. \tag{5}$$

For the sphere $\varepsilon = 1$, and C is the curvature. For the ellipsoid $\varepsilon \neq 1$ and $\varepsilon > 0$. For the hyperboloid of one sheet $\varepsilon < 0$.

ii) Paraboloid
In this case we get:

$$\alpha = r^2, \tag{6}$$

$$\beta = 1/4 r^4 C^2. \tag{7}$$

iii) Cylinder

$$\alpha = 2C^{-2}[1 - (1 - C^2 y^2)^{1/2}], \tag{8}$$

$$\beta = x^2. \tag{9}$$

Applying the third order approximation we get

$$\alpha = y^2. \tag{10}$$

The cylinder axis of revolution is positioned in the meridian plane.

   In the case of holo-lens the Gaussian image location does not depend on substrate geometry (for a holo-lens we put $x_o = x_r = 0$ and $y_o = y_r = 0$). The location of Gaussian image is given by equations:

$$V_i = V_c \pm \mu(V_o - V_r),$$

$$x_i V_i = x_c V_c,$$

$$y_i V_i = y_c V_c \tag{11}$$

where: $V_q = \gamma_q \, 1/|z_q|$, $q \in (i, c, o, r)$; z_q is the z coordinate of: image point source,

reconstruction point source, object point source, reference point source, respectively:

$$\gamma_q = \begin{cases} 1 \text{ for divergence beam,} \\ -1 \text{ for convergence beam,} \end{cases}$$

$$\mu = \lambda_2/\lambda_1$$

where λ_1 is the reference light wavelength, λ_2 is the reconstruction light wavelength. The sign "$+$" corresponds to the primary image and the sign "$-$" to the secondary image. The geometry of holo-lens substrate has influence only on spherical aberration and coma [9] (we deal with the third order aberrations). Therefore, we limit our consideration to these aberrations. The coefficients for the aberrations considered in the case of holo-lens are [9]:

$$S = V_c^3(1-C\varepsilon z_c)^2 - V_i^3(1-C\varepsilon z_i)^2 \pm \mu[V_o^3(1-C\varepsilon z_o)^2 - V_r^3(1-C\varepsilon z_r)^2], \tag{12}$$

$$G = V_c^3(1-C\varepsilon z_c) - V_i^3(1-C\varepsilon z_i) \pm \mu[V_o^3(1-C\varepsilon z_o) - V_r^3(1-C\varepsilon z_r)], \tag{13}$$

$$S_p = V_c^3 - V_i^3 \pm \mu(V_o^3 - V_r^3), \tag{14}$$

$$C_x = x_c V_c^3(1-C\varepsilon z_c) - x_i V_i^3(1-C\varepsilon z_i), \tag{15}$$

$$C_y = y_c V_c^3(1-C\varepsilon z_c) - y_i V_i^3(1-C\varepsilon z_i), \tag{16}$$

$$C_{px} = x_c V_c^3 - x_i^3 V_i^3, \tag{17}$$

$$C_{py} = y_c V_c^3 - y_i V_i^3, \tag{18}$$

S_p, C_{px}, C_{py} are of the same form as coefficients corresponding to aberrations of holo-lens recorded on a plane substrate.

Having the wavefront W_3 (Eq. (1)) we can determine the transverse aberrations δx_i, δy_i by the equations:

$$\delta x_i = -\frac{\partial W}{\partial x} z_i, \tag{19}$$

$$\delta y_i = -\frac{\partial W}{\partial y} z_i. \tag{20}$$

For the holograms recorded on the plane substrate it is easy to find analytical formulas describing the shape of aberration spot corresponding to the aberration considered [10]. For the holo-lenses recorded on the quadrics we could not find explicit formulas which allow us to recognize the shape of aberration spots. The formulas are very complicated. However, by applying the approximate formula (5) for α_a in the case of substrates considered in the point i) we are able to find analytically the shape of aberration spots for coma and spherical aberration. The expression for the spherical aberration with α_a is

$$W_s = -1/8r^4 S. \tag{21}$$

In this case

$$S = V_c^3(1-Cz_c)^2 - V_i^3(1-Cz_i)^2 \pm \mu[V_o^3(1-Cz_o)^2 - V_r^3(1-Cz_r)^2. \tag{22}$$

There is no difference in formula (21) between spherical, hyperboloidal and ellipsoidal holo-lens, because the parameter ε is reduced. Substituting (21) and (22) into (19) and (20) we get:

$$\delta x_i = 1/2xr^2Sz_i, \tag{23}$$

$$\delta y_i = 1/2yr^2Sz_i. \tag{24}$$

Applying the polar coordinate we get:

$$\delta x_i = 1/2\rho^3Sz_i\cos\Theta, \tag{25}$$

$$\delta y_i = 1/2\rho^3Sz_i\sin\Theta. \tag{26}$$

These are the parametric equations describing sphere with radius: $r_s = 1/2\rho^3Sz_i$ and with center located at the center of Gaussian image.

The expression for coma with α_a is

$$W_k = 1/2xr^2C_x + 1/2yr^2C_y. \tag{27}$$

In this case

$$C_x = x_cV_c^3(1-Cz_c) - x_iV_i^3(1-Cz_i) \text{ and } C_y = y_cV_c^3(1-Cz_c) - y_iV_i^3(1-Cz_i). \tag{28}$$

Here, as above, the parameter ε is reduced, so we cannot distinguish between the surfaces considered in our approximated theory. Substituting (27) and (28) to (19) and (20) we get:

$$\delta x_i = -1/2(3x^2+y^2)C_xz_i - xyC_yz_i, \tag{29}$$

$$\delta y_i = -1/2(3y^2+x^2)C_yz_i - xyC_xz_i. \tag{30}$$

Matching Eqs. (29) and (30) and applying the polar coordinate we get

$$\delta x_i^2 + \delta y_i^2 + 2\delta x_i\rho^2C_xz_i + 2\delta y_i\rho^2C_yz_i + 3/4\rho^4(C_x^2+C_y^2)z_i = 0. \tag{31}$$

Equation (31) corresponds to the circle with the radius $r_s = 1/2\rho^2(C_x^2+C_y^2)^{1/2}z_i$ and coordinates of the center given as $(-\rho^2C_xz_i, \rho^2C_yz_i)$.

Comparing these results with results in work [10], we can see that the considerate aberration spots are of the same shape, in the approximation (5), as the corresponding aberration spots for a plane holo-lens.

The shape of aberration spots of paraboloid holo-lens (point ii) cannot be found in such a way, because of the form of α (8) and β (9). Although it is possible to find an approximate expression for α in the case of the cylindrical substrate (point iii), the expression describing aberration spot is still too complicated. There is no symmetry between the variables x and y in expressions for α_a and β.

3. Numerical examples

In order to show the influence of the quadrics substrate on the aberration spots given by holo-lens we want to consider the holo-lens described in paper [11]. It is

a collimation holo-lens with parameters: $z_o = 100$ mm, $z_r = z_c = -\infty$, $\mu = 1$, radius of the holo-lens is equal to 10 mm. We consider the primary image $z_i = 100$ mm. The holo-lens is spherical aberration free. To get the aberration spot corresponding to spherical aberration we put $z_c = -1000$ mm, then $z_i = 111.11$ mm. For the coma we put $x_c/z_c = 0.04$.

The figures below show the size and the shape of aberration spots (each figure has its own scale) corresponding to the spherical aberration and coma. Figures 1a, b, c show the aberration spots corresponding to the spherical aberration for holo-lens recorded on
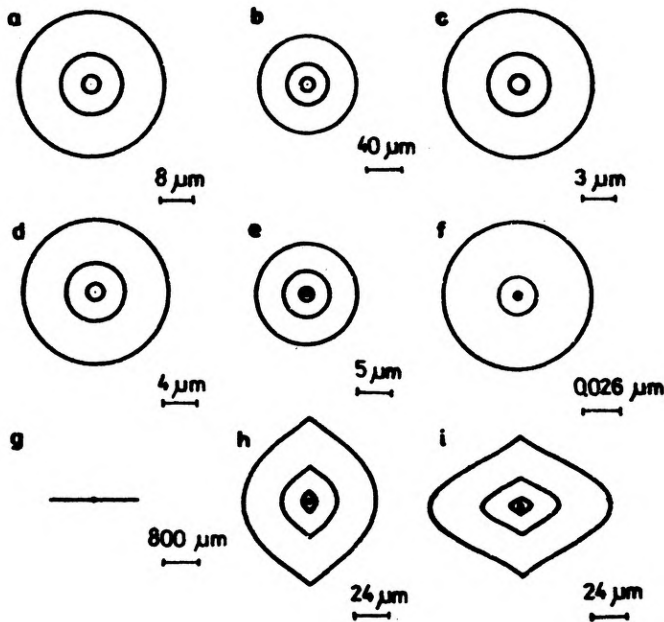

Fig. 1. Spherical aberration: **a** – plane substrate, **b** – spherical substrate ($\rho = 200$ mm), **c** – spherical substrate ($\rho = 100$ mm), **d** – ellipsoidal substrate ($\rho = 100$ mm, $\varepsilon = 8$), **e** – hyperboloidal substrate ($\rho = 100$ mm, $\varepsilon = -8$), **f** – paraboloidal substrate ($\rho = 100$ mm), **g** – cylindrical substrate ($\rho = 100$ mm), **h** – "plane-cylindrical" substrate ($\rho = 100$ mm), **i** – "cylindrical-plane" substrate ($\rho = 100$ mm)

plane substrate, spherical substrate with radius $\rho = 200$ mm, spherical substrate with radius $\rho = 100$ mm, respectively. It is worth noting that the radius $\rho = 100$ mm is optimal for the holo-lens [11]. Figures 1d, e show the aberration spots corresponding to spherical aberration for ellipsoid, hyperboloid substrate, respectively. The obtained shape confirms the conclusions from Sect. 2. Resolution of the figures is too low to show the difference between circle and real shape of the aberration spots. Figures 1f, g show the aberration spots corresponding to spherical aberration for paraboloid, cylinder substrate, respectively. In the case of paraboloid the shape is also actually circular, but the spot is much smaller than that obtained for

a plane holo-lens. In the case of cylinder we obtained practically a segment. We can notice a great size of the segment.

The aberration spots for coma are shown in Fig. 2a–g, for the same examples. The shape is rather typical except cylinder (Fig. 1f) when it is practically a segment. The holo-lens recorded on a spherical substrate with radius $\rho = 100$ mm is coma
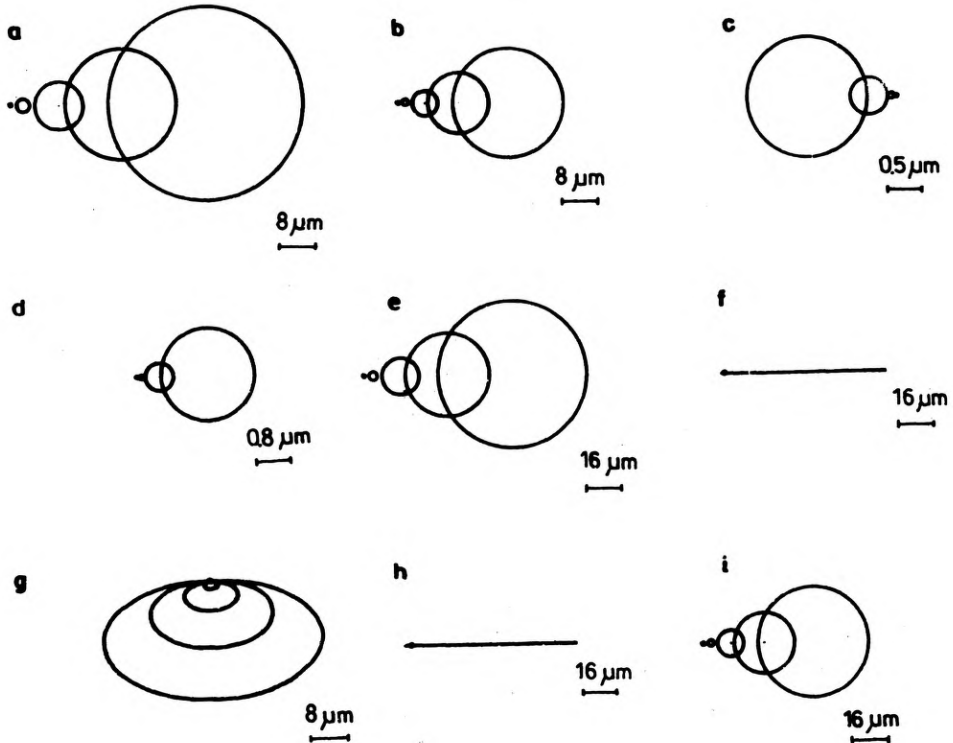

Fig. 2. Coma: **a** – plane substrate, **b** – spherical substrate ($\rho = 200$ mm), **c** – ellipsoidal substrate ($\rho = 100$ mm, $\varepsilon = 8$), **d** – hyperboloidal substrate ($\rho = 100$ mm, $\varepsilon = -8$), **e** – paraboloidal substrate ($\rho = 100$ mm), **f** – cylindrical substrate-meridian plane, ($\rho = 100$ mm), **g** – cylindrical substrate-sagittal plane ($\rho = 100$ mm), **h** – "plane-cylindrical" substrate ($\rho = 100$ mm), **i** – "cylindrical-plane" substrate ($\rho = 100$ mm)

free (there is no figure in this case). In the case of cylindrical holo-lens we included aberration spots for a meridian plane (Fig. 2f) and sagittal plane (Fig. 2g).

4. "Plane-cylindrical" holo-lens

The cylindrical holograms are easy to manufacture. That is why it is worth dealing with cylindrical holograms in more detail. We can record a hologram on a plane substrate, then bend it into cylinder with radius ρ and read it out as a cylindrical one.

Let us consider the set-up in Fig. 3. According to [9] the total wave aberration is given by:

$$W = \sum_{n=0}^{\infty} \sum_{k=0}^{n} \sum_{l=0}^{n-k} W_{n,k,l}. \tag{32}$$

The aberrations terms $W_{n,k,l}$ are of the form:

$$W_{n,k,l} = b_{n,k,l} [V_c^{2n-1} \omega_c^{n-k-l} \beta_c^l \xi_c^k - V_i^{2n-1} \omega_i^{n-k-l} \beta_i^l \xi_i^k$$
$$\pm \mu (V_o^{2n-1} \omega_o^{n-k-l} \beta_o^l \xi_o^k - V_r^{2n-1} \omega_r^{n-k-l} \beta_r^l \xi_i^k)], \tag{33}$$

$$b_{n,k,l} = (-1)^{k+1} \frac{(2n-3)!!}{(n-k-l)! \, k! \, l! \, 2^k},$$

$$\beta_q = -1/2(x_q^2 + y_q^2), \tag{34}$$

$$\omega_q = xx_q + yy_q, \tag{35}$$

$$\xi_q = r^2 + z^2 - 2zz_q. \tag{36}$$

The ξ_q contains the whole information about substrate geometry.
For the recording part $q \in (r, o)$ ξ_q is of the form

$$\xi_q = r^2. \tag{37}$$

For the reproducing part $q \in (c, i)$ ξ_q is of the form

$$\xi_q = 2C^{-2} [1 - (1 - C^2 y^2)^{1/2}](1 - Cz_q). \tag{38}$$

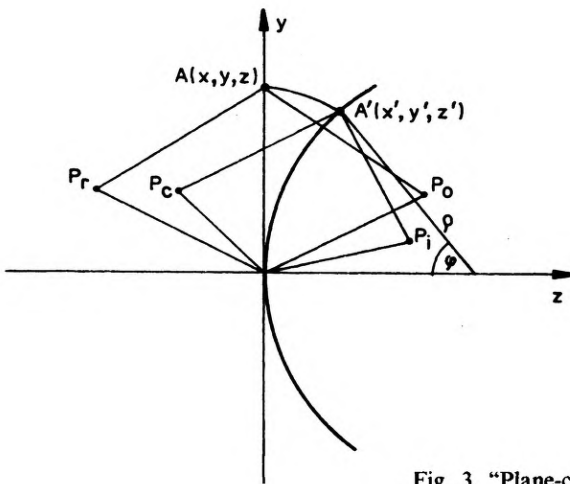In order to use formula (32) we have to find the relation between each point

Fig. 3. "Plane-cylindrical" hologram (scheme in yz plane)

$A(x, y, z)$ on the plane hologram with a point $A'(x', y', z')$ corresponding to it on the cylindrical hologram (Fig. 3). At first we can notice that $x = x'$, so it is enough to find the relation between y and y' because z and z' are related by y, y' and cylinder equation. We can see that the length of segment OA is equal to the length of arch OA$'$. Hence

$$\varphi = y/\rho \tag{39}$$

where ρ is the radius of the cylinder. Having φ we can determine y'

$$y' = \rho \sin y/\rho. \tag{40}$$

For small φ we get $y' \cong y$. Inserting (37) and (38) and putting $n = 2$ that corresponds to the third order aberration, we get the expression for the third order wave aberration of our set-up.

$$W_3 = -\frac{1}{8}\alpha_p^2 S_p' - \frac{1}{8}\alpha_c^2 S'' - \frac{1}{4}\alpha_c\beta G'' - \frac{1}{8}\beta^2 S_p'' + \frac{1}{2}x\alpha_p C_{px}' + \frac{1}{2}y\alpha_p C_{py}' + \frac{1}{2}x\alpha_c C_x''$$

$$+ \frac{1}{2}y'\alpha_c C_y'' + \frac{1}{2}x\beta C_{px}'' + \frac{1}{2}y'\beta C_{py}'' - \frac{1}{2}x^2 A_x - \frac{1}{2}y^2 A_y' - \frac{1}{2}xy A_{xy}' - \frac{1}{2}y'^2 A_y''$$

$$- \frac{1}{2}xy' A_{xy}'' - \frac{1}{4}\alpha_p F_p' - \frac{1}{4}\alpha_c F'' - \frac{1}{4}\beta F_p'' + \frac{1}{2}xD_x + \frac{1}{2}yD_y' + \frac{1}{2}y'D_y'' \tag{41}$$

where:

$$\alpha_p = r^2, \tag{42}$$

$$\alpha_c = 2C^{-2}(1 - \cos\varphi), \tag{43}$$

$$\beta = x^2. \tag{44}$$

The prim coefficients correspond to the recording part of hologram and the bis coefficients correspond to the reproduced part of hologram. For example:

$$S_p' = \pm\mu(V_o^3 - V_r^3), \tag{45}$$

$$S_p'' = \pm\mu(V_c^3 - V_i^3), \tag{46}$$

$$S'' = V_c^3(1 - Cz_c)^2 - V_i^3(1 - Cz_i)^2. \tag{47}$$

The expression for the transverse aberration of the "plane-cylindrical" holo-lens is even more complicated than for cylindrical holo-lens. Figure 1h shows the aberration spot for spherical aberration and Fig. 2h shows the aberration spot for coma in the case of collimation holo-lens used in the previous examples. The spherical aberration is similar in size to that for a plane holo-lens but it is not a circle. The coma has the same size and shape as coma for cylindrical holo-lens.

5. "Cylindrical-plane" holo-lens

We can also record a hologram on a cylinder, straighten it into a plane and

reproduce as a plane hologram. Following the method from Sect. 4 we get

$$
W_3 = -\frac{1}{8}\alpha_c^2 S' - \frac{1}{4}\alpha_c\beta G' - \frac{1}{8}\beta^2 S_p' - \frac{1}{8}\alpha_p^2 S_p'' + \frac{1}{2}x\alpha_c C_x' + \frac{1}{2}y'\alpha_c C_y' + \frac{1}{2}x\beta C_{px}'
$$

$$
+ \frac{1}{2}y'\beta C_{py}' + \frac{1}{2}x\alpha_p C_{px}'' + \frac{1}{2}y\alpha_p C_{py}'' - \frac{1}{2}x^2 A_x - \frac{1}{2}y'^2 A_y' - \frac{1}{2}xy' A_{xy}' - \frac{1}{2}y^2 A_y''
$$

$$
- \frac{1}{2}xy A_{xy}'' - \frac{1}{4}\alpha_c F' - \frac{1}{4}\beta F_p' - \frac{1}{4}\alpha_p F_p'' + \frac{1}{2}xD_x + \frac{1}{2}y'D_y' + \frac{1}{2}yD_y''. \tag{48}
$$

Figures 1i, 2i show aberration spots for spherical aberration and coma, respectively. The spherical aberration is similar to that obtained for a "plane-cylindrical" in Sect. 4. The coma is similar to that obtained for a plane holo-lens.

6. Final remarks

Comparing figures corresponding to spherical aberration (Fig. 1c–e) and coma (Fig. 2c–d) for spherical, ellipsoidal, and hyperboloidal substrate, we can see that the shape of aberration spot is the same and the size of it is very similar to each other. This fact is in agreement with our theoretical results presented in Sect. 2, in which using the approximate formula (5) we showed that for substrate listed above we got the same expression for the third order eikonal corresponding to spherical aberration (21) and coma (27). Thus, in the third order approximation each of the substrates considered can be replaced by a sphere with curvature C. The spots given in Fig. 2c and 2d can be approximated by a point, which corresponds to the spot for spherical holo-lens with the same value of parameter C (coma is compensated for this value of C). The fact that for a paraboloidal substrate the shape of aberration spot is also similar to the shape of aberration spots for a spherical substrate cannot be a general conclusion for all the cases, because we have not any general analytical formula as it was in the previous case.

Because it is easy to perform cylindrical holo-lenses we showed formulas for the third order aberration of: cylinder, "plane-cylindrical" and "cylindrical-plane" holograms. The formulas we have got are very intricate, so we are not able to investigate the aberration spots analytically. The examples of aberration spots for the spherical aberration and coma (Fig. 1h–i and 2h–i) are not encouraging. The shape of aberration spot corresponding to spherical aberration is not as interesting as for the cylindrical holo-lens (Fig. 1f) and it is greater than the spot for spherical holo-lenses. However, our results cannot be generalized for reasons given for paraboloidal holo-lens.

We do not insert the aberration spots corresponding to the very non-technological quadrics.

The character of the numerical methods made us restrict our paper to choose one example instead of general consideration. We chose well described holo-lens.

In order to get better description of the influence of the substrate geometry on the

image quality, we have to perform some new numerical investigations without the third order approximation. This problem will be the subject of the next paper.

References

[1] Welford W. T., Opt. Commun. **9** (1973), 268.
[2] Champagne E. B., J. Opt. Soc. Am. **57** (1967), 51.
[3] Meier R. W., J. Opt. Soc. Am. **55** (1965), 987.
[4] Jagoszewski E., Optik **49** (1985), 85.
[5] Mustafin K. S., Opt. Spektrosk. **37** (1974), 1198.
[6] Peng K., Frankena A. J., Appl. Opt. **25** (1986), 1319.
[7] Lagasse P. E., Verboven P. E., Appl. Opt. **25** (1986), 4150.
[8] Masajada J., Nowak J., Opt. Appl. **20** (1990), 177.
[9] Masajada J., Nowak J., Appl. Opt. **30** (1991), 1791.
[10] Nowak J., Opt. Appl. **10** (1980), 245.
[11] Zając M., Nowak J., Gadomski A., Opt. Appl. **2** (1989), 229.

Аберрационные пятна третьего порядка голографических линз, полученных на поверхностях второго порядка

Исследованы аберрационные пятна для сферической аберрации и комы голографических линз, полученных на поверхностях второго порядка. Анализ был проведен численным и, по мере возможности, аналитическим методами. Были найдены формулы аберрации третьего порядка для голограмм, полученных на плоской поверхности и загнутой в цилиндр во время реконструкции. Были также исследованы аберрационные пятна голографических линз.

Проверил Станислав Ганцаж